

Optimizing Bunsen burner Performance Using CFD Analysis

Aruna Devadiga¹, Prof. Dr. T. Nageswara Rao²

¹M. Tech Student, Oxford College of Engineering, Bangalore – 560068, Karnataka

²Professors, Department Of Mechanical Engineering, Oxford College of Engineering,
Bangalore– 560068, Karnataka

ABSTRACT: Industry relies on heat from the burners in all combustion systems. Optimizing burner performance is critical to complying with stringent emissions requirements and to improve industrial productivity. Even small improvements in burner energy efficiency and performance can have significant impacts in a continuous operation, more so if the improvements can be used in other combustion systems and across industries. While tremendous advances have been made in understanding the fundamentals of combustion, the remaining challenges are complex. To make improvements, it is critical to understand the dynamics of the fuel fluid flow and the flame and its characteristics. Computational Fluid Dynamics offers a numerical modelling methodology that helps in this regard. In the existing work, valid computational models are used for the study of different modes of combustion and also to study the mixing of fuel and air inside the burner mixing chamber to obtain the optimum Air to Fuel ratio. Liquefied petroleum gas (LPG) which has a composition of Propane and Butane in the ratio 60:40 by volume, is used as the fuel. Bunsen burner is used for the experiments. The present work has attempted to establish the validity of the Computational results by conducting appropriate experiments. The first series of simulations were done for proper mixing of fuel-air in the mixing chamber of burner. These were done for different mass flow rates of the fuel. Variation in the mass flow rates resulted in variation of the flame lengths, flame velocity, and temperature profiles across the flame. The second stage included the modelling and meshing of the combustion zone (assumed to be cylindrical in shape) with different number of grid points to check the accuracy of the mesh and also to see the variation in the results obtained from solver. The results obtained from the mixing chamber are the values which are input to the combustion chamber. These results are in the ratio of air to fuel mixture, mass flow rate of the mixture, velocity, mass fractions of oxygen, propane and butane separately. The combustion zone results were analysed for variations in temperature, mass fractions of propane, butane, oxygen, carbon dioxide, carbon monoxide, at different heights. Pressure and velocity variations were also studied for different mass flow rates. The experimental part consisted of measuring the temperature profile of the flame obtained from the burner at different mass flow rates. Prior to this, the calibration of the rota meter was also done. The rota meter was used to obtain different flow rates of the fuel. With the experiments, combustion phenomena like flame lift, blow off and flash back can be observed and the corresponding flow rate can be input to the computations to study these phenomena using CFD. CFD provides more scope for study and analyses of the results than the experiments. The experimental results are compared with those of computational results and they are in close proximity to the CFD results. The deviation of the experimental results from the CFD obtained results are due to non ideal working conditions during the experiments. The results obtained from computations provide an estimate of Equivalence ratio, reactant and product concentrations in the flame, temperature, turbulence, inlet and outlet velocity of fuel-air mixture etc. These studies cannot be conducted experimentally and hence computational results are used to establish the validity and also for in depth study of the dynamics of Combustion.

I. INTRODUCTION

Combustion is the most important process in engineering, which involves turbulent fluid flow, heat transfer, chemical reactions, radioactive heat transfer and other complicated physical and chemical phenomena. Typical engineering applications include internal combustion engines, power station combustors, boilers furnaces etc. It is important to study the different modes of combustion taking place in these instruments, chemical kinetics involved, temperature and flame velocity, mass flow rate of the fuel etc to improvise the working of these equipments and maximising the efficiency.

The different modes of Combustion are premixed combustion, diffusion combustion and mixed mode combustion. In premixed combustion air and fuel are premixed to the required stoichiometry before burning. In the diffusion mode, a diffusion flame may be defined as a non-premixed, quasisteady, nearly isobaric flame in which most of the reaction occurs in a narrow zone that can be approximated as a surface. In the mixed mode combustion there is partial premixing of flames as well as diffusion also occurs. Such flames occur in many practical applications like in industrial burners, gas-fired domestic burners, rocket burners and also gas turbine combustors. Although flows in combustors usually are turbulent, analyses of flame stabilization are often based on equations of laminar flow. This may not be as bad as it seems because in the regions of the flow where stabilization occurs, distributed reactions may be dominant, since reaction sheets may not have had time to develop; an approximation to the turbulent flow might then be obtained from the laminar solutions by replacing laminar diffusivities by turbulent diffusivities in the results.

The important combustion phenomena which have received considerable attention in the recent years are Flame lift-off mechanisms, lift-off height, lift-off velocity and blow off velocity. Study of these phenomena helps to fix the operating range or operating limits of a burner. We are studying these phenomena using different flames using a Bunsen burner at different mass flow rates of the fuel and simulating the data using time accurate, higher order numerical methods with detailed transport and chemistry models using ANSYS ICEM CFD software. Combustion modelling is done using ANSYS ICEM CFD software. This software uses Reynolds Average Navier Stokes Equations (RANS) to solve the continuity equations of mass, momentum and energy. Numerical flow simulation, or more common Computational Fluid Dynamics

(CFD), relies on solving conservation or transport equations for mass, momentum, energy and participating species. If the flow is turbulent, model equations for specific turbulent quantities have to be solved in addition. Since even with today's super computers resolving turbulent length scales directly results in tremendous effort, Reynolds averaged equations are applied to include the physics of turbulence. To discretize and solve the governing flow equations Finite Volume method is employed by the majority of commercial CFD codes.

II. METHODOLOGY

Methodology involves experimental analysis and CFD analysis. The complexity of combustion modelling was the challenging module of this entire work. In turbulent combustion one distinguishes between premixed, non-premixed and partially premixed combustion. The problem was initiated by taking the case of a most simple burner which is used in most engineering applications, the Bunsen burner. Prior to the combustion analysis, proper mixing of the fuel and air was analysed in the mixing chamber of the Bunsen burner by using the software ANSYS ICEM CFD and CFX solver. Selection of the appropriate turbulence model for the mixing of fuel in the mixing chamber is crucial. This was a direct consequence of the Air/Fuel ratio at the outlet of the burner, and hence played a crucial role in the formulation of the combustion phenomena occurring in the combustion zone. The nature of turbulent flow is irregular with rapid fluctuations in velocity, temperature, pressure, density and composition. This fluctuating nature makes turbulent flow highly diffusive resulting in enhanced transport of momentum, mass and energy. The Eddy Dissipation Model was selected in the CFX solver which is best suited for solving turbulent conditions as it uses the Reynolds Average Navier Stokes model to solve the equations. The results obtained from the solver are analysed with respect to variation of different properties like temperature, pressure, velocity, mass fractions. The same are compared at different number of grids to optimise the number of grid points. For the experiments, Liquefied Petroleum Gas (LPG) is used as the fuel and the ratio of mass fractions of propane: butane taken is 0.53: 0.47. The kinetics of LPG combustion is established and the validation of these results is done by measuring the temperature profile of the flame of the Bunsen burner. The CFD analysis is especially used to establish the flow dynamics in the burner and also to explain the different variations of properties inside the flame.

III. EXPERIMENTAL ANALYSIS OF FLAME TEMPERATURE AT GIVEN FUEL FLOW RATE

Liquid petroleum gas (LPG) is used as the fuel for Bunsen burner. The LPG composition has 60% propane and 40% butane by volume. The flow is controlled by a precision regulator and is measured using a rota meter. The flow rate must be kept constant for one full set of readings of the flame temperature. The rota meter least count is 10ml/min. The maximum flow rate that can be measured by this rota meter which is used for the experiments is 400ml/min. The scope of the experiment is to ensure that the assumptions in the computational and mathematical modelling are valid and not irrational. The aim of the experiment was to obtain the temperature profile in the flame, and match the experimental results to the computational results obtained. By doing this, the combustion model used, and chemical kinetics can be justified.

The aim is to measure the temperature of the flame along the length of the flame in both x and y axes. A travelling microscope is modified to traverse along x and y axes. It consists of a longitudinal and latitudinal slot with markings on it like a vernier scale. The connecting frame moves in the slots and this movement is caused by operating two motors with the help of battery or power box. The power box is used to supply constant voltage of 3.5 volts. This helps the thermocouple to traverse at constant speed. A fine thermocouple (Platinum-Platinum Rhodium-13%) is attached to the arm of the instrument which traverses along the x and y axes of the flame and measures the temperature. The thermocouple is connected to a power box which helps to maintain a constant velocity of traverse by keeping the voltage constant. With the help of a data acquisition, the temperature measured by the thermocouple is recorded in a computer. The software is preloaded in the computer and the time for which the temperature is to be recorded is set for 100ms which means for every 100 milliseconds the temperature data is recorded. The flow is controlled by a precision regulator and is measured using a rota meter. The flow rate must be kept constant for one full set of readings of the flame temperature. When a steady flame is achieved the flame is scanned at different heights. Care should be taken to keep the flame steady. Also, the fuel flow rate should be closely monitored, since any change in the flow rate can directly affect the flame height, and hence the kind of flame attained. Keeping in mind all these factors, steady readings were recorded and plotted.

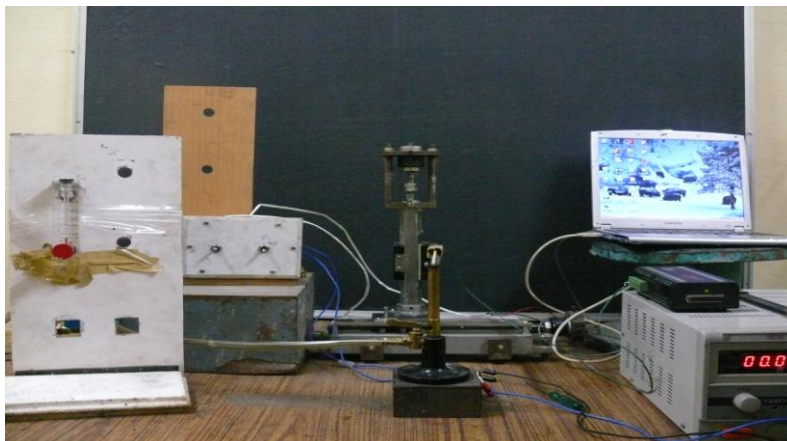


Figure 3.1 Experimental setup for recording Flame Temperature

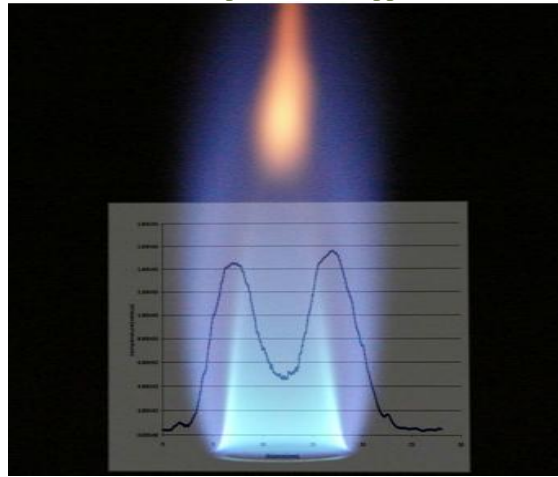


Figure 3.2 Temperature profiles at fuel mass flow rate 100ml/min

The figure 3.2 shows the temperature profile being overlapped on the flame. The temperature was recorded at 100ml/min flow rate at 2cm above the burner rim. The flame is axisymmetric and hence the temperature graph is also axisymmetric. At the burner ends it can be observed that the temperature is less due to heat transfer to the cold walls of the burner. The highest temperature is recorded at the edge of the inner cone, as the mixture gets adequate amount of oxygen for the complete combustion of fuel-air mixture. At the centre of the flame there is drastic dip in temperature. This is because the rich mixture from the mixing chamber which comes out like a jet lacks sufficient oxygen for combustion. Hence there is incomplete combustion in this region leading to formation of carbon monoxide.

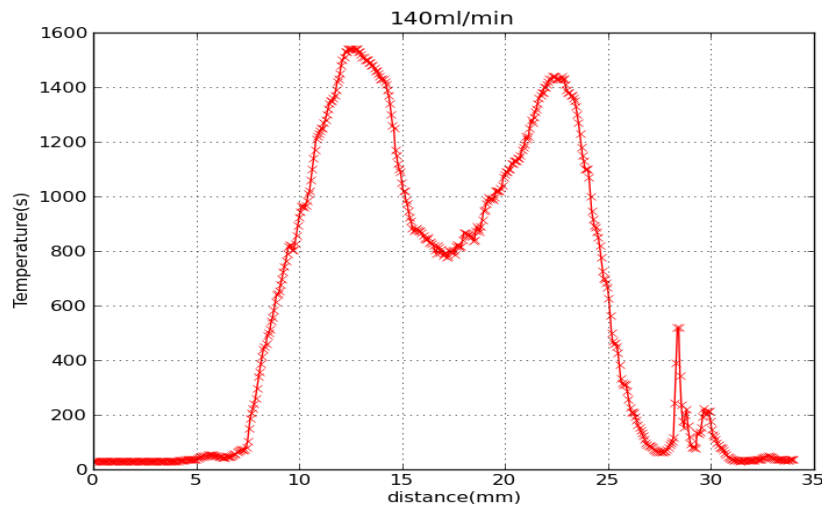


Figure 3.3 Bunsen Flame Temperature profile at flow rate of 140ml/min

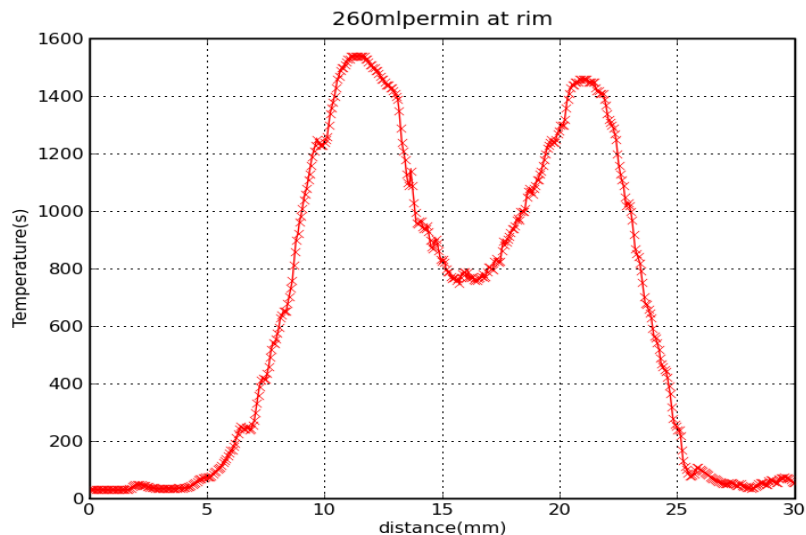


Figure 3.4 Bunsen Flame Temperature profile at flow rate of 260ml/min

IV. CFD ANALYSIS OF FLAME TEMPERATURE AT A GIVEN FUEL FLOW RATE

For CFD analysis of the Bunsen burner mixing chamber and the Combustion Zone, the details of the conditions specified for each of these domains are specified here. The modelling and meshing of geometries are done using the ANSYS ICEM CFD software and is imported to the CFX solver for pre processing and post processing. The Computational modelling is done for the burner mixing chamber and then for the combustion zone. The modelling and meshing techniques are used. The pre-processor consists of modelling and meshing of the geometry. The Burner mixing chamber is modelled using ANSYS ICEM CFD and the meshing is done using structured meshing technique. The length of the mixing chamber is taken to be equal to 100mm. The outlet rim diameter is equal to 10mm. The fuel inlet diameter is set to be equal to 1mm. Axisymmetric case is considered for the modelling of mixing chamber. Once the geometric modelling is done, mesh or grids should be generated for the model. This involves dividing the whole geometry into number of equally spaced volumes or cells. This process is termed as discretization. This discretization should be done in such a way that the continuity of the process variables from one cell to another should be maintained throughout the whole geometry. Structured meshing techniques are used for mesh generation, as structured meshing gives better results than unstructured meshing.

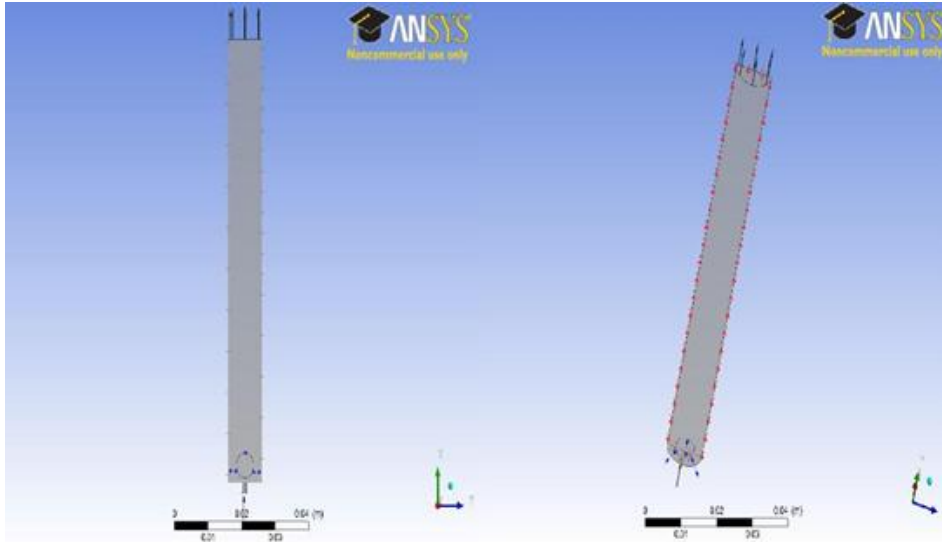


Figure 4.1 Bunsen burner mixing chamber geometric modelling (axisymmetric) showing air and fuel inlet, outlet in ANSYS CFX

Boundary Conditions are specified in the CFX solver as follows

<p>Default Domain:</p> <ol style="list-style-type: none"> Fluid = Liquefied Petroleum Gas(LPG) Reference Pressure = 1 atm Turbulence Model = k-ε Model Temperature = 300K Constraint Component = N2 	<p>Fuel Inlet:</p> <ol style="list-style-type: none"> Boundary Type = Inlet Mass Fraction C3H8 =.53 Mass Fraction C4H10 =.48 Relative Pressure = 0.0001 bar
<p>Air Inlet:</p> <ol style="list-style-type: none"> Boundary Type = Opening Mass Fraction C3H8 =0 Mass Fraction C4H10 =0 Mass Fraction O2 =.232 Flow Direction = Normal to Boundary Condition 	<p>Outlet:</p> <ol style="list-style-type: none"> Boundary Type = Outlet Mass and Momentum = Average Static Pressure Relative Pressure = 0 bar
<p>Solver Criteria:</p> <ol style="list-style-type: none"> Advection Scheme: High Resolution Maximum Iterations: 10000 Residual Target: 1e-7 	

V. BURNER MIXING CHAMBER RESULTS

The post processing results of the Mixing Chamber give variation of propane, butane, oxygen, outlet mixture mass flow rate, air to fuel ratio, velocity of the fuel air mixture at the outlet etc.

Fuel flow Rate (g/s)	C3H8 mass fraction	C4H10 mass fraction	Mass flow rate at outlet	Velocity of fuel at outlet (m/s)	Oxygen mass fraction	Velocity of air at Air-inlet (m/s)	Velocity of Fuel at fuel-inlet (m/s)
140	.115867	.10275	8.21214e-5	1.61207	.181619	2.4321	19.356
220	.115095	.102066	9.92093e-5	1.94883	.181811	3.20962	26.9487
260	.114877	.101872	11.5964e-5	2.27898	.181712	3.845	31.4304

Table 5.1 CFX solver Post processing results of the Burner mixing chamber at different mass flow rates.

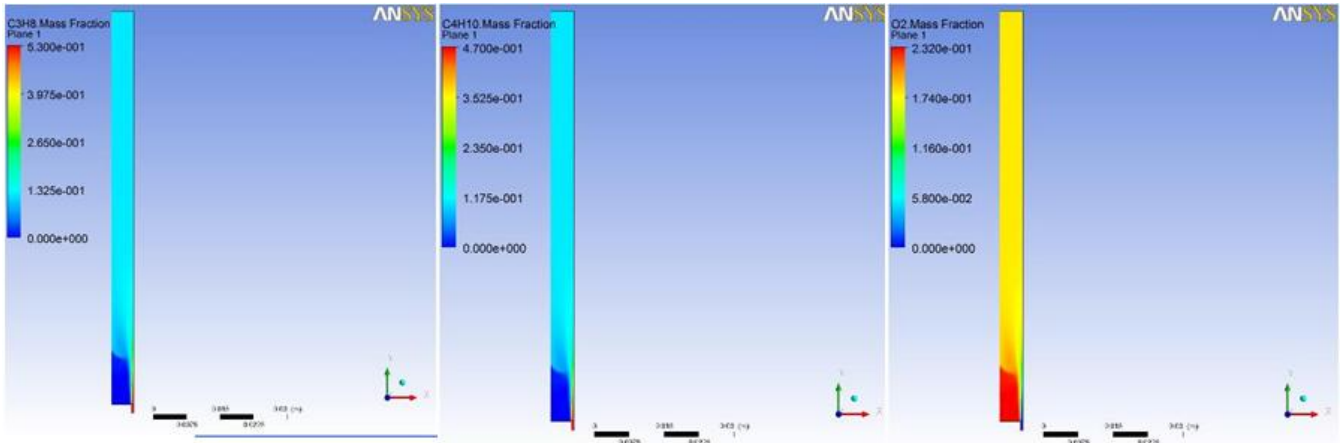


Figure 5.1 Mass fraction variation of propane, butane and oxygen (from top left, clockwise) separately in the burner mixing chamber as obtained from ANSYS CFX solver.

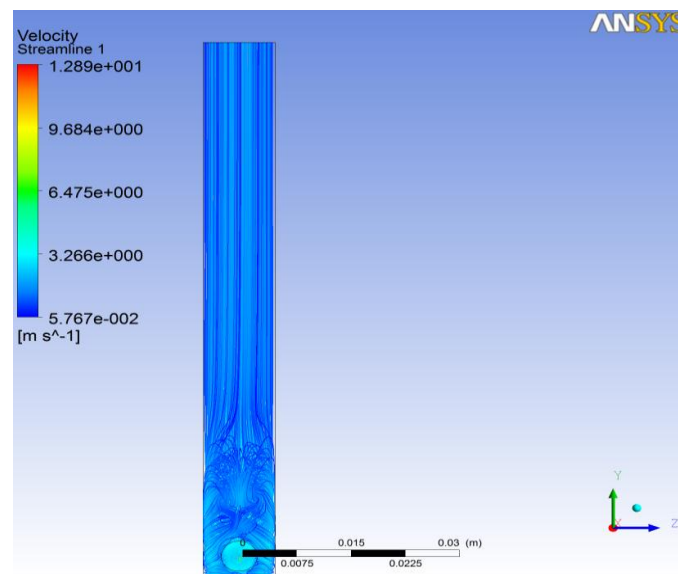


Figure 5.2 Air-Fuel mixtures velocity streamlines showing the velocity profile inside the burner mixing chamber

VI. MODELLING AND ANALYSIS OF THE COMBUSTION ZONE

The combustion zone modelling was done using ANSYS ICEM CFD. A section of the cylindrical combustion zone was modelled with angle of 45 degrees in between as shown in the figure. The vertical length of the combustion chamber is 200mm and the horizontal length is 50mm. The meshing was done using structured meshing technique. The results obtained from the mixing chamber are given as input conditions to the combustion chamber. The parameters selected for the input file to the combustion zone are velocity, mass fraction and mass flow rates. A dense grid is assigned carefully in and around the central fuel jet where large gradients are expected. To avoid singularity at centre in axisymmetric case of 45 degrees, a quarter O grid is used near the fuel jet. Mesh quality has been checked for grid skewness to ensure good convergence. The quality of the grid obtained is 65% and total number of nodes generated is 5, 00,000. Grid independent studies are also made for comparing and validating the results.

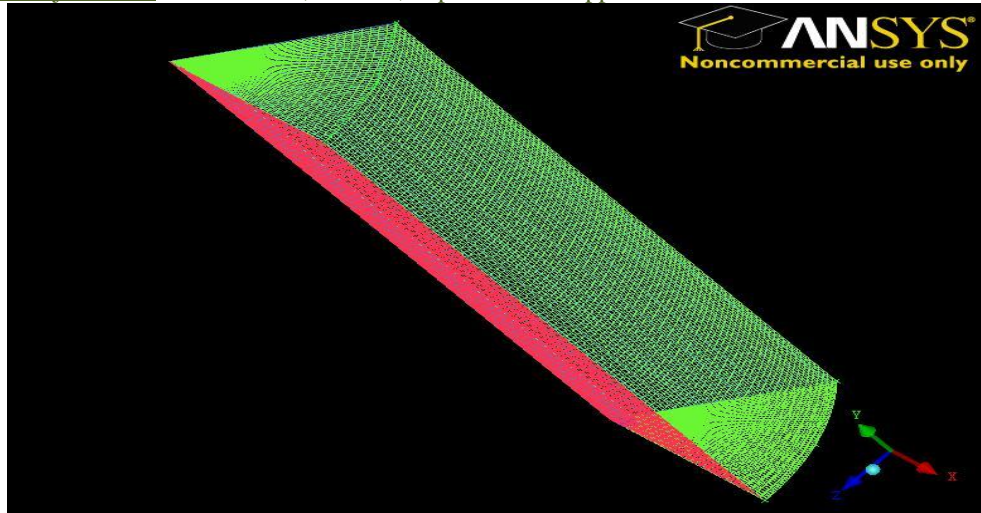


Figure 6.1 Sectioned Combustion Zone with structured meshing done in ANSYS ICEM CFD

Boundary Conditions for Combustion Zone:

The boundary conditions vary for different mass flow rates and are obtained from the result files (.res format). A situation is raised wherein a heat source needs to be modelled to initiate combustion. This heat source should not add to the heat generated by the flame and also this heat source should exist in a defined volume and for specified time duration. This is done by modelling a step function for the temperature near the inlet domain to be 900 K for time duration of 0.1s.

Step Function –CEL Code:

LIBRARY:

CEL:

EXPRESSIONS:

Temp Func = 300[K]+600[K]*step(0.005-z/1[m])*step(0.005-y/1[m])*step(0.1- t/1[s])

END

END

This serves as the ignition source for the combustible mixture at the outlet of the Bunsen burner.

The Boundary Conditions are:

<p>Default Domain:</p> <ul style="list-style-type: none"> a. Fluid = LPG b. Heat transfer Model = Thermal Energy c. Reference pressure = 1 atm d. Turbulence Model = k-ε model e. Combustion Model = eddy dissipation Model 	<p>Material Creation:</p> <ul style="list-style-type: none"> a. Material created = LPG mixture b. Mixture properties = Reacting Mixture c. Material Group = Gas Phase Combustion d. Additional Material List = CO, CO2, H2O, N2, O2 e. Reaction List = Butane Air WD2, Propane Air WD2
<p>Inlet Conditions:</p> <ul style="list-style-type: none"> a. Boundary Type = Inlet b. Flow regime = Subsonic c. Fuel flow speed = Velocity corresponding to different flow rates d. C3H8 Mass Fraction = n.a e. C4H10 Mass Fraction = n.a f. O2 Mass Fraction = n.a 	<p>Outlet Conditions:</p> <ul style="list-style-type: none"> a. Flow regime = subsonic b. O2 Mass Fraction = 0.232 <p>Solver Criteria:</p> <ul style="list-style-type: none"> a. Advection Scheme: High Resolution b. Maximum Iterations: 30000 c. Residual Target: 1e-7
<p>Symmetry Conditions applied to the remaining parts of the domain for symmetry calculations along the domain, as explained above.</p>	

A second order accurate scheme is used for spatial discretization with physical advection terms. A time step of 1e-7 is used with 30000 iterations and the solutions is aid to be converged. The boundary conditions are specified for the combustion zone at different mass flow rates. For each mass flow rate, the mass fractions of butane, propane, oxygen and inlet mass flow rate of the fuel-air mixture, velocity (which are the outlet results of burner mixing Chamber) change.

VII. ANALYSIS OF COMBUSTION ZONE AT DIFFERENT MASS FLOW RATES

In this section, the post processing results obtained for combustion Zone at different flow rates are analysed. The variation of different properties like mass fractions, temperature, pressure, velocity and their effect on the flame can be studied.

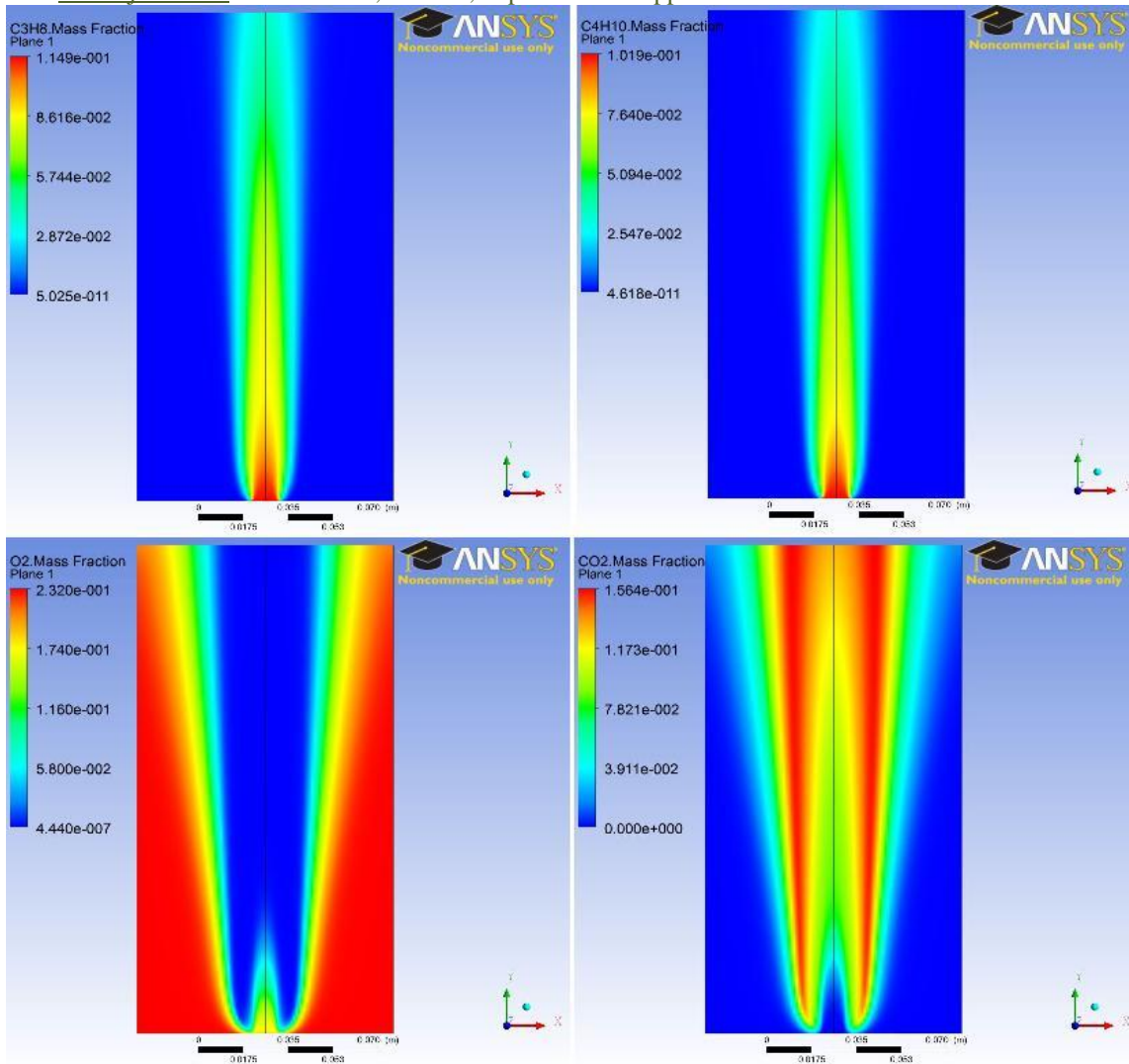


Figure 7.1 Variation of C3H8, C4H10, O2, CO2 in the Combustion Chamber at flow rate of 260ml/min

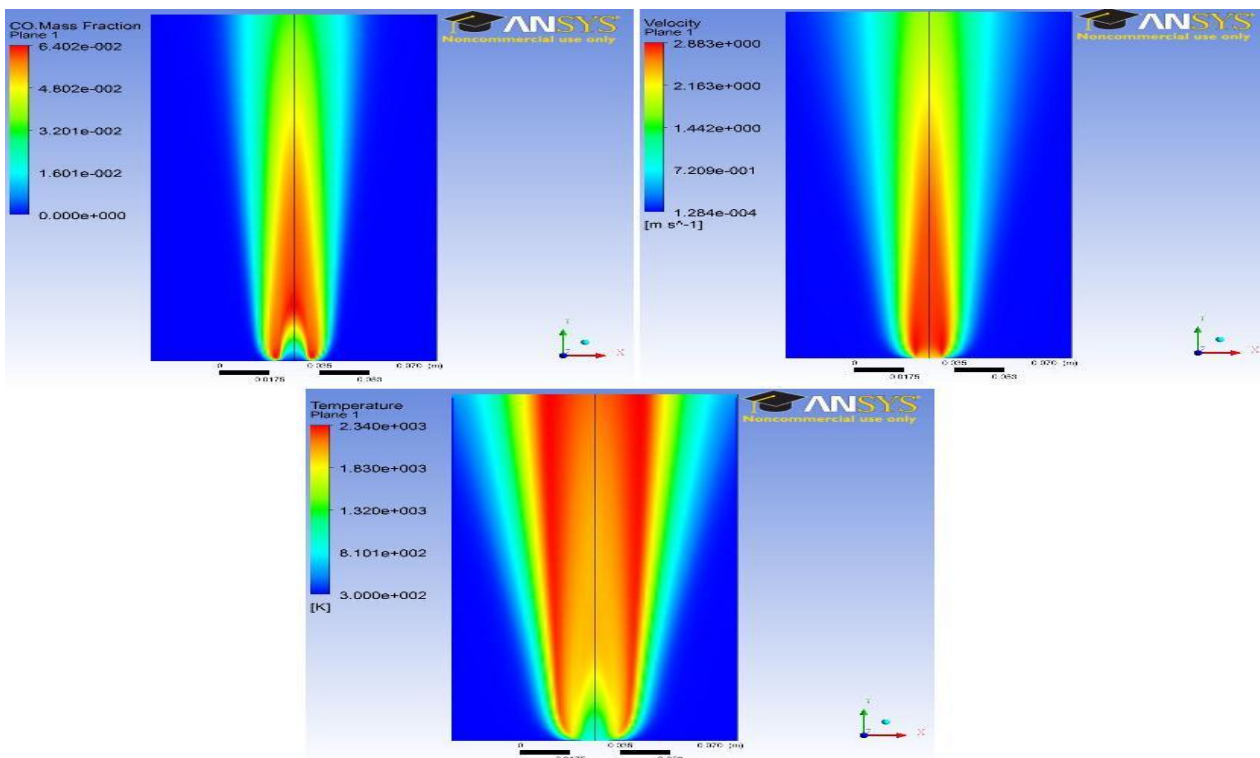


Figure 7.2 Variation of CO, Velocity, Temperature in the Combustion Chamber for flow rate of 260ml/min

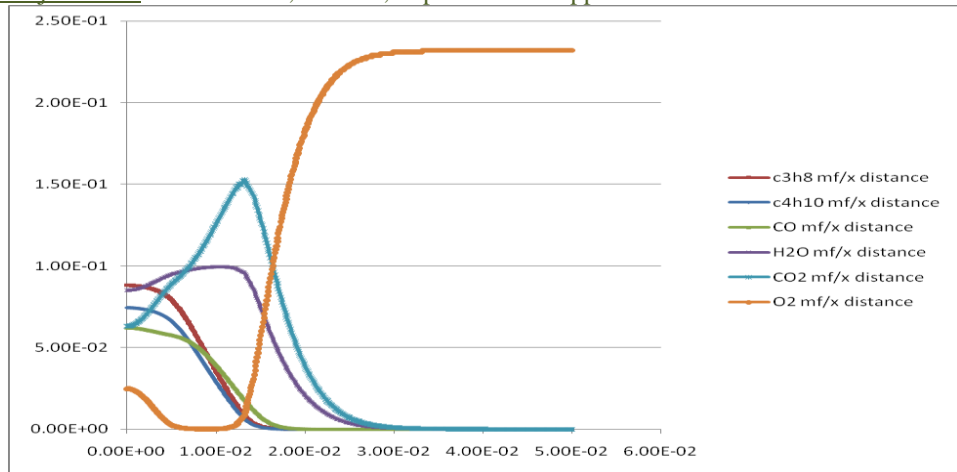


Figure 7.3 Variation of Mass Fractions of reactants and products inside the combustion zone for flow rate of 260ml/min

As it can be seen from the figure 7.3, the propane and butane mass fractions are decreasing from the centre and the consumption of oxygen rapidly increases between 10mm to 20mm from the centre and is the highest beyond 20mm as the availability of ambient oxygen is more. The CO₂ composition increases first which shows that complete combustion occurs. Beyond 15mm from the centre the CO₂ composition decreases which indicates that though there is oxygen available there is scarcity of the fuel beyond this point. This is also indicated by the rapid decrease in compositions of propane and butane beyond this point. There is presence of carbon monoxide only within 10mm from the centre which indicates that due to rich fuel- air mixture in that area incomplete combustion has occurred leading to formation of carbon monoxide.

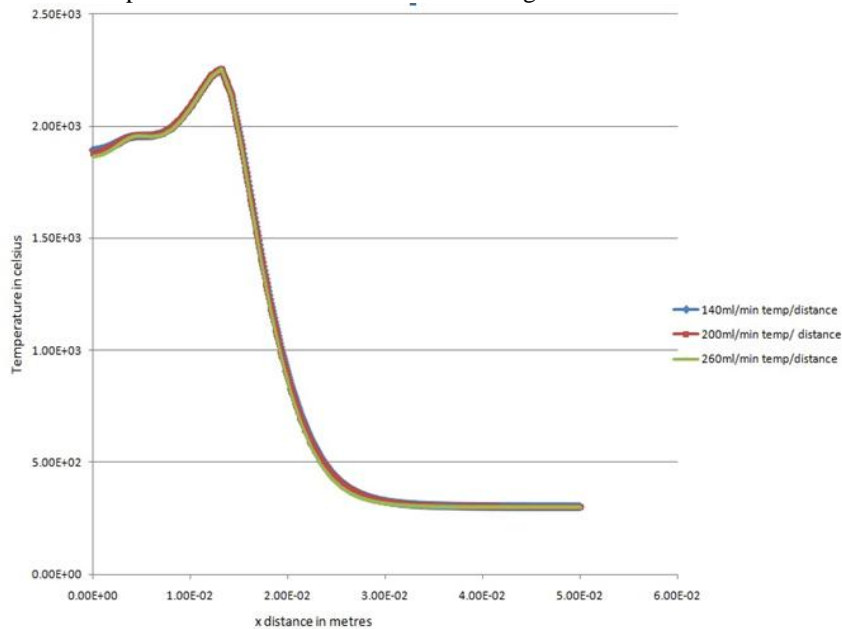


Figure 7.4 Temperature profiles in combustion zone at different flow rates read from CFX solver

In the figure 7.4, the temperature profiles of flames at all the flow rates are same, which indicates that the profiles of the flame at any flow rate which is similar as obtained in CFX solver. Comparing the profiles to the CO₂ profile in the figure 7.3, it can be observed that the trend of the graphs is the same. This CO₂ concentration indicates that there is complete oxidation taking place of the reactants, which results in increase in heat release rate. Hence, it can be said that temperature varies with the variation of CO₂.

VIII. RESULTS AND DISCUSSIONS

Here, comparisons between the experimental and computational results are made and studied. Comparisons are made for different properties like mass fractions, temperature, etc and these are validated. The validations are also done by comparing with results of other research papers which have also established similar results.

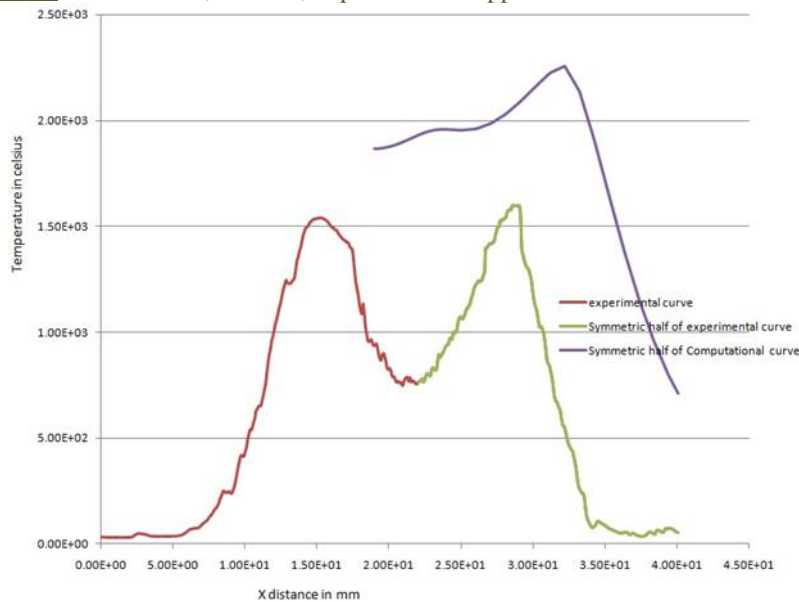


Figure 8.1 Comparison of experimental and computational temperature profiles at 260ml/min

The experimental curve is an axisymmetric curve which is obtained from the thermocouple traverse along the wholly length of the flame. But in the computational results it is not possible to obtain an axisymmetric curve as the measurement is made along the line extending from the centre of the combustion chamber to wall of the combustion chamber. This discrepancy in the measured temperature is attributed to uncertainties in the measurements and the model (e.g. related to the chemical mechanism and the thermo physical and transport properties). The high-temperature region appears to be slightly narrower in the laboratory flame due to burner edge effects. This will be corroborated by the species concentration measurements. The hotter regions do not necessarily correspond to regions of high chemical activity, because the heat released in the reaction zones is transported both upstream (by diffusion) and downstream to other portions of the flame. In both the measurements and predictions, the region with the highest temperatures lies between the inner premixed and the central non premixed reaction zone. The basic structure of the flame can be assumed to consist of distinct layers that include 1) an inner layer (PF) in which hydro carbon fuel and O₂ consumption occur and 2) an oxidation layer (NF) (surrounded by a preheat zone downstream of PF and a post flame zone downstream of NF). All of the hydrocarbon chemistry can be assumed to occur in the inner layer where fuel and radical consumption occurs to form CO and H₂. In the oxidation layer, the CO and H₂ formed in the inner layer are oxidized to form CO₂ and H₂O. The CO-oxidation layer is generally thicker than the H₂-oxidation layer, and the overall thickness of the oxidation layer itself is, in general, greater than that of the inner layer. Furthermore, the heat release is primarily due to the exothermic reactions occurring in the oxidation layer. A major exothermic reaction in the oxidation layer $\text{NF/CO} + \text{OH} = \text{CO}_2 + \text{H}$ occurs on a relatively slower. Time scale than either the initiation reactions in the inner layer (PF), e.g., $\text{CH}_4 + \text{H} = \text{CH}_3 + \text{H}_2$, (in case methane is used) or the other major oxidation reaction in the NF, namely, $\text{H}_2 + \text{OH} = \text{H}_2\text{O} + \text{H}$. Thermocouple losses can also be accounted for the variation in temperature measurement. These are discussed in brief here. The thermocouple has become one of the most used instruments to measure this quantity. Although the devices are inexpensive, convenient and easy to use, there can be significant errors associated in temperature measurements when used in fire environments. If these errors are acknowledged and sensors are designed and used judiciously, the temperature measurement can be estimated with much greater accuracy. Most errors associated with the use of thermocouples are due to the fact that the temperature of the sensor may not be the temperature of the surrounding medium. Energy can be transferred to and from the bead of the thermocouple by radiation, convection and conduction. Unfortunately, when placed in the high intensity environments characteristic of fires, thermocouples can produce sensed temperatures significantly different than the actual temperature of the medium of interest. These errors can be attributed to variations in the rate of energy transfer to and from the TC bead, temperature variations along the lead wires, and catalytic reactions between the metals comprising the bead at the surrounding gases.

Radiant heat transfer from the temperature sensor to its surroundings can be a large source of error. The law governing radiation from an emitter is the Stefan-Boltzman law defined as: $\text{grad} = \epsilon\sigma T^4$ where ϵ is the emissivity of the object and σ is the Stefan-Boltzman constant ($\sim 5.669 \times 10^{-8} \text{ W}\cdot\text{m}^{-2} \cdot \text{K}^{-4}$). Since radiation is proportional to T^4 , it is obvious that at high temperatures a thermocouple bead could be radiating much more energy that it is receiving. This is especially true when the surrounding environment is at a much lower temperature and not emitting radiation to the bead, which is common in fire environments. To compound the problem, a large radiant energy source is present as well. When the flame is in close proximity to the sensor it radiates energy that may increase the temperature of the bead significantly over that of the gas surrounding the sensor. The thermal radiation losses from the hot flame to the cold walls of the burner amount to maximum heat loss.

Energy is transferred to the surface of the bead from the gas flowing around it by convection. This mode of heat transfer is more efficient when the fluid has a high velocity and is the basis for aspirated thermocouples. The relative contributions of radiant and convective energy transfer to the thermocouple measurement vary with the application.

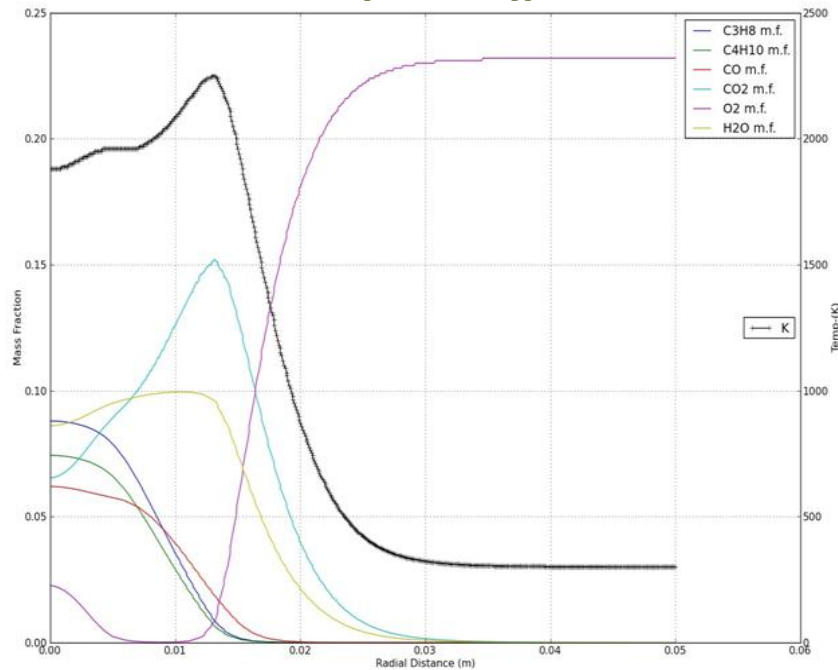


Figure 8.2 Comparisons of Mass Fraction profiles with temperature profile at 260ml/min along x-axis of the flame as obtained from CFX solver.

In the above figure 8.2, it can be seen that the trend of temperature variation and CO₂ mass fraction variation are similar. This observation suggests that when complete oxidation takes place, the reactants are converted into CO₂ and H₂O and the heat energy release peaks at this point. This results in temperature peak at the same point. Another observation made from the figure 8.2 is that the oxygen is at the lowest point when the temperature and CO₂ are at their peak values. This suggests that all the available oxygen was consumed for the complete oxidation of the reactants.

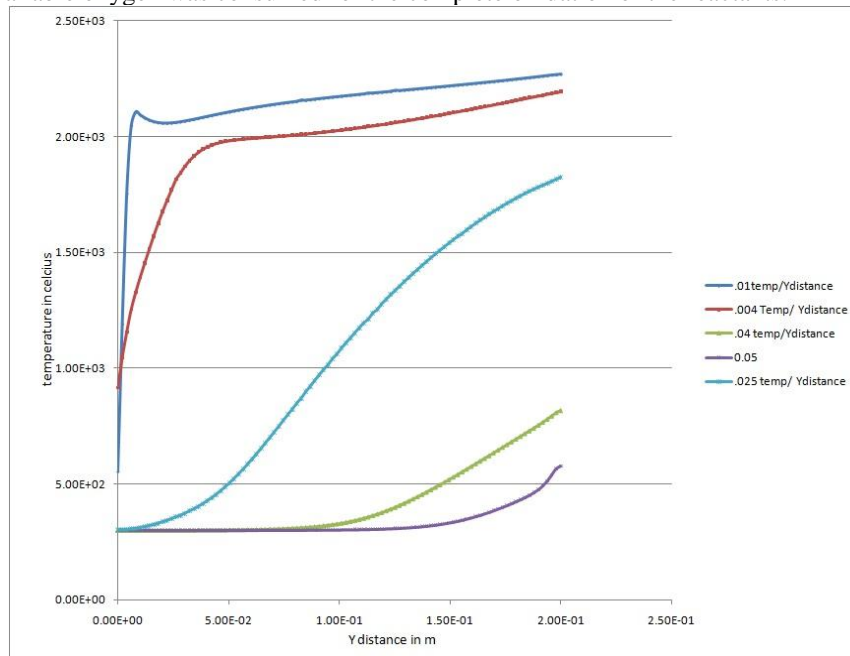


Figure 8.3 Variations of Temperature at different points in the flame along Y axis from centre of combustion zone at 260ml/min

From the figure 8.3, the temperature shows increasing trend at .004 m and .01 m from the centre and goes on decreasing then on for .025m, .04m and .05m. The part of the flame up to .01m is called the inner layer in which oxidation process occurs. Due to chemical reactions taking place in this region, there is heat release occurring which results in increase in temperature. The part of the flame up to .004 m is called the inner layer where all of the hydrocarbon chemistry can be assumed to occur where fuel and radical consumption occurs to form CO and H₂. In the oxidation layer, which starts from a little beyond .04m and stretches up to .01m, the CO and H₂ formed in the inner layer are oxidized to form CO₂ and H₂O. It can be seen in the later part that CO formation is more at x= .004 m than at x= .01m from the centre along y. This explains presence of CO₂ in this region at .01m compared to other regions as shown figure 8.5

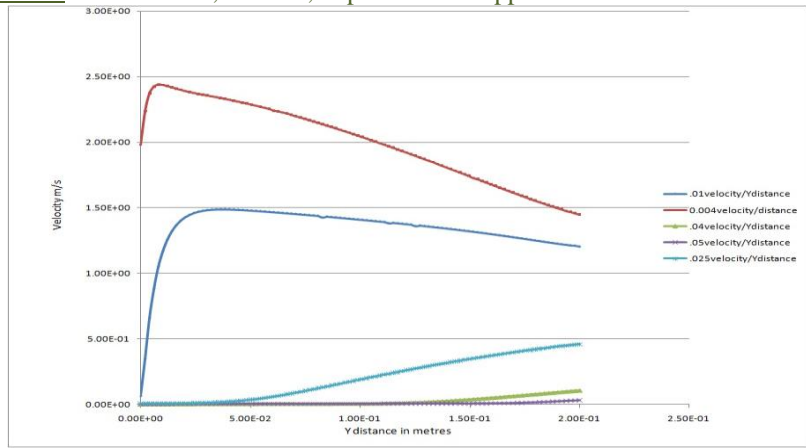


Figure 8.4 Variations of Velocity at different points in the flame along Y axis at 260ml/min

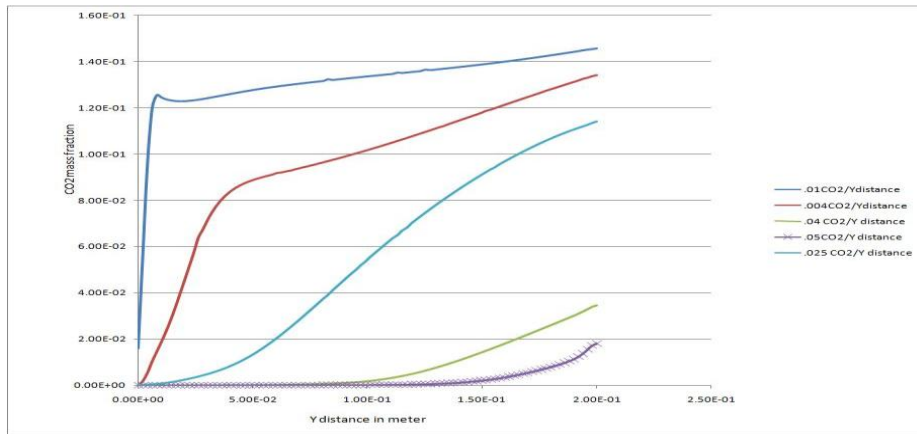


Figure 8.5 Variations of CO2 mass fraction at different points in the flame along Y axis at 260ml/min

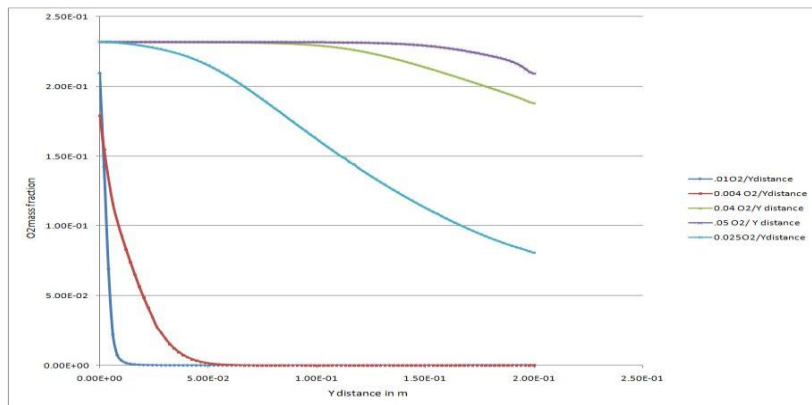


Figure 8.6 Variations of O2 mass fraction at different points in the flame along Y axis

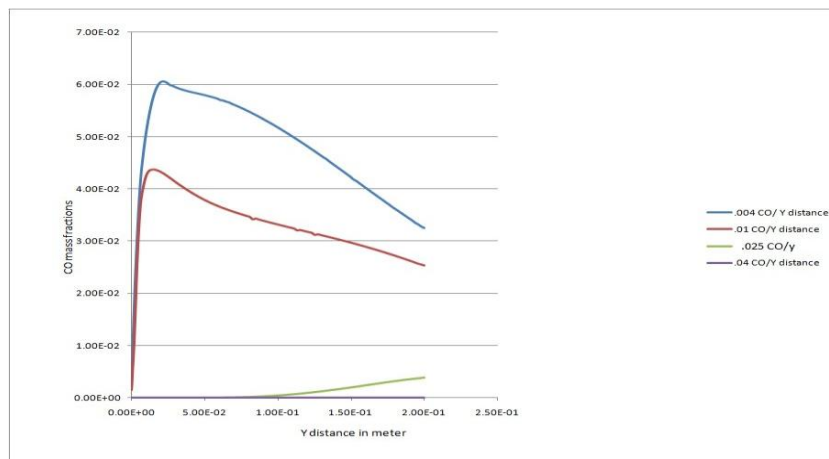


Figure 8.7 Variations of CO mass fraction at different points along Y axis

Comparing the figures 8.5 and 8.6, it is seen that as O₂ decreases, CO₂ increases. At $x = .025\text{m}$ distance and beyond that, it is seen that there is excess O₂ available from the ambient atmosphere, but is not consumed due to scarcity of fuel in this region. The chemical reactions do not occur in this region due to the presence of lean mixture, and even if they do occur they are incomplete. As seen from the figure 8.5, the concentration of carbon oxide is high at $x = .004\text{m}$ as this region of the flame comprises of the inner layer where complete oxidation does not take place. At $x = .01\text{m}$ distance, which comprises of the oxidation layer where conversion of CO is converted to CO₂. Hence, as shown in figure 8.5, the concentration of CO₂ is high at $x = .01$ than at $x = .004\text{m}$.

IX. CONCLUSIONS

The products obtained in the combustion process, adiabatic flame temperature, flame length, degree of diffusion flame, are all a direct function of the stoichiometry. The flame structure is obtained in the form of instantaneous snapshots of the flow at various times. In the fuel-rich annular ring, the same initiation process is dominated by premixed combustion close to the nozzle exit. As oxygen is depleted inside the annular ring, the excess fuel emerging from the fuel-rich premixed zone is transported outward (by convection and diffusion), and non premixed flames are established on both sides of the annular ring. The two high-temperature product regions later merge into a single surface in the plume. Subsequently, the buoyant acceleration of hot gases outside the diffusion flame surface causes shear layer rollup, leading to the formation of toroidal vortex rings, which then interact with the flame/plume surface. The basic structure of the flame can be assumed to consist of distinct layers include 1) An inner layer in which methane and O₂ consumption occur and 2) An oxidation layer (surrounded by a preheat zone downstream of inner layer and a post flame zone downstream of oxidation layer). All of the hydrocarbon chemistry can be assumed to occur in the inner layer where fuel and radical consumption occurs to form CO and H₂. In the oxidation layer, the CO and H₂ formed in the inner layer are oxidized to form CO₂ and H₂O. The CO-oxidation layer is generally thicker than the H₂-oxidation layer, and the overall thickness of the oxidation layer itself is, in general, greater than that of the inner layer. Furthermore, the heat release is primarily due to the exothermic reactions occurring in the oxidation layer. A major exothermic reaction is in the oxidation layer. $\text{CO} + \text{OH} = \text{CO}_2 + \text{H}$ occurs on a relatively slower timescale than either the initiation reactions in the inner layer. e.g., $\text{CH}_4 + \text{H} = \text{CH}_3 + \text{H}_2$, or the other major oxidation reaction in the oxidation layer, namely, $\text{H}_2 + \text{OH} = \text{H}_2\text{O} + \text{H}$. Partially premixed flames are hybrid flames containing multiple reaction zones. These flames are of fundamental importance to the phenomena of non premixed flame stabilization and liftoff, spray combustion, and localized extinction zone is established in between these two wings ~in the region where excess fuel and oxidizer from the rich and lean premixed reaction zones, respectively, mix in stoichiometric proportion. The overall flame structure is determined by the interactions between these three reaction regions, and can be controlled by changing the various reactant velocities and equivalence ratios. A fundamental difference between a partially premixed flame and an equivalent premixed or non premixed flame pertains to the existence of multiple synergistically coupled reaction zones. The structure of partially premixed flames is determined by the interactions that arise among these zones due to the synergy between the thermo chemistry and the heat and mass transport. For example, in a methane-air triple flame the inner rich premixed reaction zone provides CO and H₂, which serve as "intermediate fuels," and excess methane to the non premixed zone, whereas the latter supplies heat and radical species ~H and OH! to both the inner and outer zones. The outer zone in turn provides excess O₂ and oxygen atoms to the non premixed reaction zone. The interactions between the various reaction zones occur due to the advection and diffusion of both heat and mass. The experimental measurement values of temperature and Computational predictions are in agreement, though the highest temperature recorded in computational predictions is 2200 Celsius where as experimental values show highest temperature to be 1600 Celsius. Discrepancy in the measured temperature is attributed to uncertainties in the measurements and the model (e.g., related to the chemical mechanism and the thermo physical and transport properties). The various graphs obtained from the computational post processing results show variations of concentrations of reactants and products in the flame at different points and also temperature and velocity fluctuations which are in excellent agreement to various theories and concepts established in the combustion. In the CFD analysis, the highest temperature recorded is the adiabatic flame temperature for LPG. The radiation losses are not taken into account here. But in experiments, the major losses occur due to heat losses from the flame to the cold walls of the burner. The high-temperature region appears to be slightly narrower in the laboratory flame due to burner edge effects. This will be corroborated by the species concentration measurements. In both the measurements and predictions, the region with the highest temperatures lies between the inner premixed and the central non premixed reaction zone.

X. FUTURE WORK

Primary recommendation to the existing work would be to introduce detailed chemistry into the solver and solve for more species in the combustion zone. Introduction of detailed chemical kinetics would affect the temperature profile to an extent and also the computational flame established. The quality of the mesh for the mixing chamber could be improved by introducing additional hexahedron elements at the air inlets and fuel inlets to capture viscous layers flow phenomenon in detailed. Some modifications need to be introduced in conducting the experiments. Different types of fuel could be used and the flames obtained, temperature data could be analysed. Attempts should be made to calculate the mass flow rate or the velocity of air entering the burner. The further step would be to carry out the experiments of flame analysis at different air-to-fuel ratios. The temperature data obtained for flame at different equivalence ratios would take us step ahead in reaching our goal of setting up of the operating limits.

REFERENCES

- [1]. J. Warnatz, U. Maas, R. W. Dibble, 'Combustion-Physical and chemical fundamentals', 4th edition, 2000, Springer.com.
- [2]. Suresh K. Aggarwal and Ishwar K. Puri, 'Flame Structure Interactions and State Relationships in an Unsteady Partially Premixed Flame', University of Illinois at Chicago, Chicago, Illinois 60607-7022
- [3]. Riccardo Azzoni, Stefano Ratti, Ishwar K. Puri, and Suresh K. Aggarwal, 'Gravity effects on triple flames: Flame structure and flow instability', University of Illinois at Chicago, Department of Mechanical Engineering (M/C 251), 842 W. Taylor St. RM 2039 ERF, Chicago, Illinois 60607-7022.
- [4]. Andrew J. Lock, Alejandro M. Briones, Xiao Qin, Suresh K. Aggarwal, Ishwar K. Puri, Uday Hegde, 'Liftoff characteristics of partially premixed flames under normal and microgravity conditions', *Combustion and Flame* 143 (2005) 159–173, www.elsevier.com/locate/combustflame.
- [5]. SANDIP GHOSAL and LUC VERVISCH, 'Stability Diagram for Lift-Off and Blowout of a Round Jet Laminar Diffusion Flame', Northwestern University, Mechanical Engineering, Evanston, IL 60208-311 USA, INSA de Rouen and CNRS-Coria UMR 6614, France.
- [6]. F.A. Williams, *Combustion Theory*, second ed., The Benjamin Publishing, 1985.
- [7]. D.B. Spalding, 'A theory of inflammability limits and flame quenching', *Proc. Roy. Soc. London. A* 240 (1957) 83.
- [8]. J. Adler, 'One-dimensional laminar flame propagation with distributed heat losses: thin-flame theory', *Combust. Flame* 7 (1963) 39.
- [9]. Y.B. Zeldovich, F.L. Barenblatt, V.B. Librovich, G.M. Makhviladze, 'The Mathematical Theory of Combustion and Explosion', Nauka ed. Moscow, 1980.
- [10]. B. J. Lee, S. H. Chung, 'Stabilization of Lifted Tribrachial Flames in a Laminar Nonpremixed Jet', Department of Mechanical Engineering, Seoul National University, Seoul 151-742, Korea.
- [11]. N. K. Aluri & S. Muppala & F. Dinkelacker, 'Large-Eddy Simulation of Lean Premixed Turbulent Flames of Three Different Combustion Configurations using a Novel Reaction Closure', Springer Science Business Media B.V. 2007
- [12]. Andrew J. Lock, Alejandro M. Briones, Xiao Qin, Suresh K. Aggarwal, Ishwar K. Puri, Uday Hegde, 'Liftoff and Extinction characteristics of Fuel and Air-stream-diluted-Methane-air flames', *Combustion and Flame* 143 (2005) 159–173, www.elsevier.com/locate/combustflame.